ACS APPLIED NANO MATERIALS

www.acsanm.org Letter

Annealed $Ti_3C_2T_z$ MXene Films for Oxidation-Resistant Functional Coatings

Xiaofei Zhao, Dustin E. Holta, Zeyi Tan, Ju-Hyun Oh, Ian J. Echols, Muhammad Anas, Huaixuan Cao, Jodie L. Lutkenhaus,* Miladin Radovic,* and Micah J. Green*

Cite This: *ACS Appl. Nano Mater.* 2020, 3, 10578−10585 Read Online

ACCESS | Metrics & More | Article Recommendations | Supporting Information

ABSTRACT: Two-dimensional transition metal carbide and nitride nanomaterials, known as MXenes, exhibit low chemical stability in aqueous environments; they tend to oxidize and react with water molecules, resulting in structural degradation and decreased electrical conductivity. This significantly limits their storage lifetime and potential use in the presence of water, particularly in nanosheet-assembled films for battery electrodes and functional coatings. Here we demonstrate that thermal annealing of $Ti_3C_2T_z$ films at elevated temperatures (~600 °C) causes changes in the termination distribution as well as the formation of a protective layer of TiO_2 on the outermost layer of films. The induced chemical and structural changes during thermal treatment arrest MXene oxidation and enable the MXene films to be stable in aqueous solutions for over 10 months.

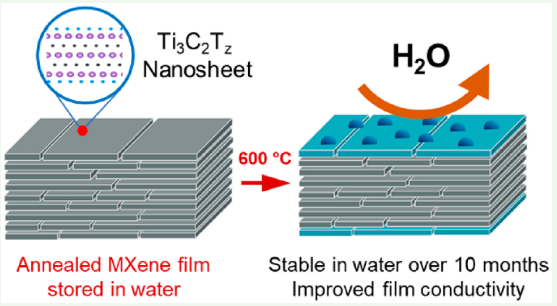

KEYWORDS: *MXenes, stabilization, Ti_3C_2, functional coatings, oxidation, thermal annealing, RF response*

MXenes are a family of 2D layered transition metal carbides, carbonitrides, and nitrides with the general chemical formula of $M_{n+1}X_nT_z$, where M represents an early transition metal such as Ti, V, Nb, Cr, and Mo; X is C and/or N; T refers to terminal groups; n ranges from 1 to 5; and z reflects the number of terminal groups.[1−5] MXenes with a multilayered structure (MXene clay) are typically synthesized by a top-down selective etching step in fluoride-containing acid (i.e., HF) to dissolve and extract an A layer from their MAX counterpart, where A refers to a group 13 or 14 element, such as Al and Si.[6,7] Single- or few-layered MXene nanosheets, which are one to a few nanometers thick, can be further derived by exfoliation of these multilayered MXene structures by agitation or sonication.[7−11] One of the most-studied members in the family of MXenes, $Ti_3C_2T_z$, is terminated with numerous functional groups (-OH, -O-, -F, and -Cl) during etching and exfoliation in the aqueous phase. Terminal groups such as -OH and -O- enable MXene nanosheets' hydrophilicity and surface electronegativity, making them readily dispersible in water and certain polar organic solvents. Freestanding films made from $Ti_3C_2T_z$ have shown promise in flexible energy storage devices such as supercapacitors,[2,12,13] portable electronics,[14] electromagnetic interference shielding coatings,[15] and gas-separation membranes.[16] The wide range of applications are enabled by MXenes' excellent electrical conductivity, abundant surface functionalities, metallic properties, in-plane stiffness, and large-scale processability by filtration, blade coating, spray coating, layer-by-layer coating, and drop-casting methods.[7,17−19]

However, MXene nanosheets oxidize rapidly in aqueous and humid environments, resulting in the degradation of the 2D structure into transition metal oxides and carbon residues, which precludes many of the properties that make MXenes-made devices attractive.[19−21] Early reports claimed that $Ti_3C_2T_z$ nanosheets react with dissolved oxygen in water and fully oxidize within just 15 days.[22] More recent studies, including our own, revealed that MXenes are prone to react with water molecules rather than dissolved oxygen.[19,21] In addition, freestanding MXene thin films also suffer from oxidation and loss of functional performance, but at a slower rate than in the dispersed form. Rapid decreases in the electronic conductivity and growth of TiO_2 nanocrystals were observed on $Ti_3C_2T_z$ films stored in humid air.[19,23,24]

This limited lifetime for MXene devices has prompted a search for strategies to mitigate MXene oxidation and degradation. A number of studies have focused on slowing down MXene oxidation by controlling the storage conditions and restricting the exposure of MXenes to water and oxygen.[19,20,22,25−27] In addition, oxidation can be mitigated by introducing antioxidants such as ascorbate and polyphosphoric anions.[28,29] Lee et al. reported that reducing $Ti_3C_2T_z$ by

Received: October 26, 2020
Accepted: November 2, 2020
Published: November 10, 2020

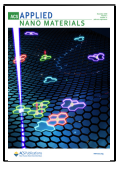

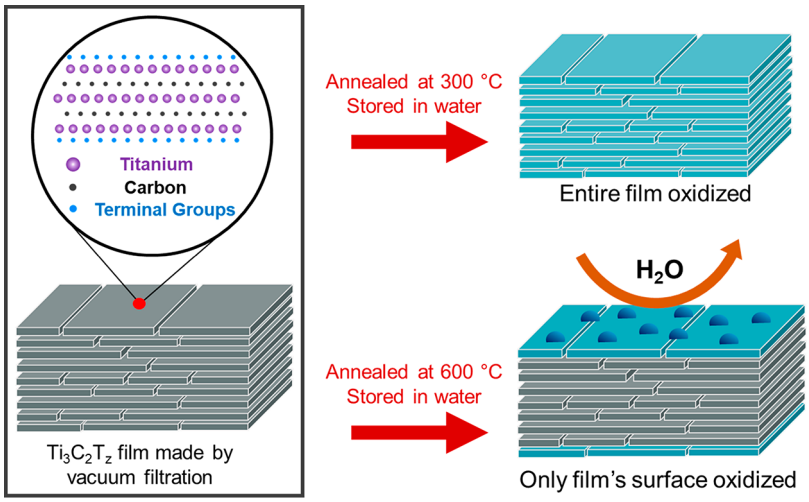

Figure 1. Schematic of $Ti_3C_2T_z$ film preparation. Films were made by vacuum filtering $Ti_3C_2T_z$ MXene nanosheets and then annealing at high temperatures under argon. Annealed MXene films were stored in distilled water for 10 months. The films annealed at 300 °C were completely oxidized and degraded. The films annealed at 600 °C only show oxidation on the surface; the oxidized layer acts as a barrier for water penetration and protects the inner layers of the film.

H_2 annealing can mitigate the oxidation of MXene film.[23] They reported that the TiO_2 formed by MXene oxidation could be reduced by H_2 gas at elevated temperatures. They also found that the fresh MXene films annealed in a H_2 environment have even slower oxidation rates in humid environments. However, the enhanced stability of MXene films was solely attributed to its reaction with H_2; the effect of structural alterations brought up by thermal annealing on film stability was not addressed. In addition, the long-term stability of annealed MXene films that are immersed in water has not been discussed in prior studies.

In this study, we demonstrate that thermally annealing freestanding MXene films under inert argon gas can induce surface and structural modifications which increase the chemical stability of the films and extend their storage life in water. Through annealing, a sandwich-like film structure was developed, with the formation of a protective TiO_2 layer on the films' surfaces and more compact nanosheet stacking that prevents water ingress and degradation of the interior structure, shown schematically in Figure 1. As-prepared $Ti_3C_2T_z$ films were annealed at 300 and 600 °C, respectively, to address the differences in stability caused by low and high annealing temperatures. In contrast to the fully degraded untreated $Ti_3C_2T_z$ film and films annealed at 300 °C, almost no changes in chemical structure and composition were observed in films annealed at 600 °C, even after 10 month storage in water. This method allows MXene thin films to have an extended lifetime and be used in a range of environments.

$Ti_3C_2T_z$ nanosheets (Figure 2a) were first derived from Ti_3AlC_2 following prior methods; we use the in situ HF method with a solution of LiF and HCl as etchant, followed by intercalation and delamination (sonication) steps.[6,7,30,31] MXene films used in this work were prepared by vacuum filtration of nanosheet dispersions through a poly(ether sulfone) filter; these films were dried under vacuum and peeled off from the polymeric filter (Figure 2b). The freestanding films were heated and annealed at either 300 or 600 °C in a tube furnace under argon flow. Before heating, the quartz tube was purged with desiccated high-purity argon for 36 h to remove trapped air and water molecules. After annealing, films were transferred into DI water and stored for 10 months.

X-ray diffraction, XRD, indicates the structural transformation from Ti_3AlC_2 MAX phase to $Ti_3C_2T_z$ nanosheets by the shift of the (002) XRD peak from $2\theta = 9.8°$ to $2\theta = 6.0°$ (Figure 2c). After annealing at 600 °C, the (002) peak shifted slightly back from $2\theta = 6.0°$ to $2\theta = 8.7°$ (Supporting Information Figure S1), suggesting a decreased interlayer spacing which may be caused by the loss of bonded water and terminal groups.[32] Anayee et al. and Persson et al. discovered that annealing MXenes up to 600 °C results in the release of intercalated and bonded H_2O, H_2, OH, CO_2, CH_4, and HF.[1,33] The absence of these attached or desorbed species caused the nanosheet stacking to become more compact. After the 10 month storage in water, MXene film previously annealed at 600 °C retains the pronounced (002) peak; however, the (002) peaks completely vanish for unannealed and 300 °C annealed films. Instead, (101) and (110) peaks appear, indicating the formation of anatase TiO_2 and rutile TiO_2, respectively, suggesting the complete oxidation and degradation of unannealed and 300 °C annealed films.[34,35] We observed that $Ti_3C_2T_z$ films become less flexible and more brittle after annealing and storage, likely due to the reduced number of functional groups. Functional groups can act as a "mortar" between nanosheet "bricks", similar to terminal group behavior for graphene oxide (GO).[36,37] This may potentially limit the films' performance in particular applications.

$Ti_3C_2T_z$ films annealed at elevated temperatures did not show significant changes in appearance compared to as-prepared films (Figure 2d,e). However, after 10 month storage in DI water, films annealed at 300 °C turn cloudy white, while the samples annealed at 600 °C did not show any noticeable difference in appearance, as it is shown in Figure 2f,g. The color change of the films suggests that the MXene film annealed at 300 °C fully degraded in water after the 10 month storage. MXenes typically degrade and lose properties in water within a month.[19−22] However, MXene films annealed at 600 °C remained gray-black, with no visible changes in color before and after storage. This is remarkable because MXene films can

https://dx.doi.org/10.1021/acsanm.0c02473
ACS Appl. Nano Mater. 2020, 3, 10578−10585

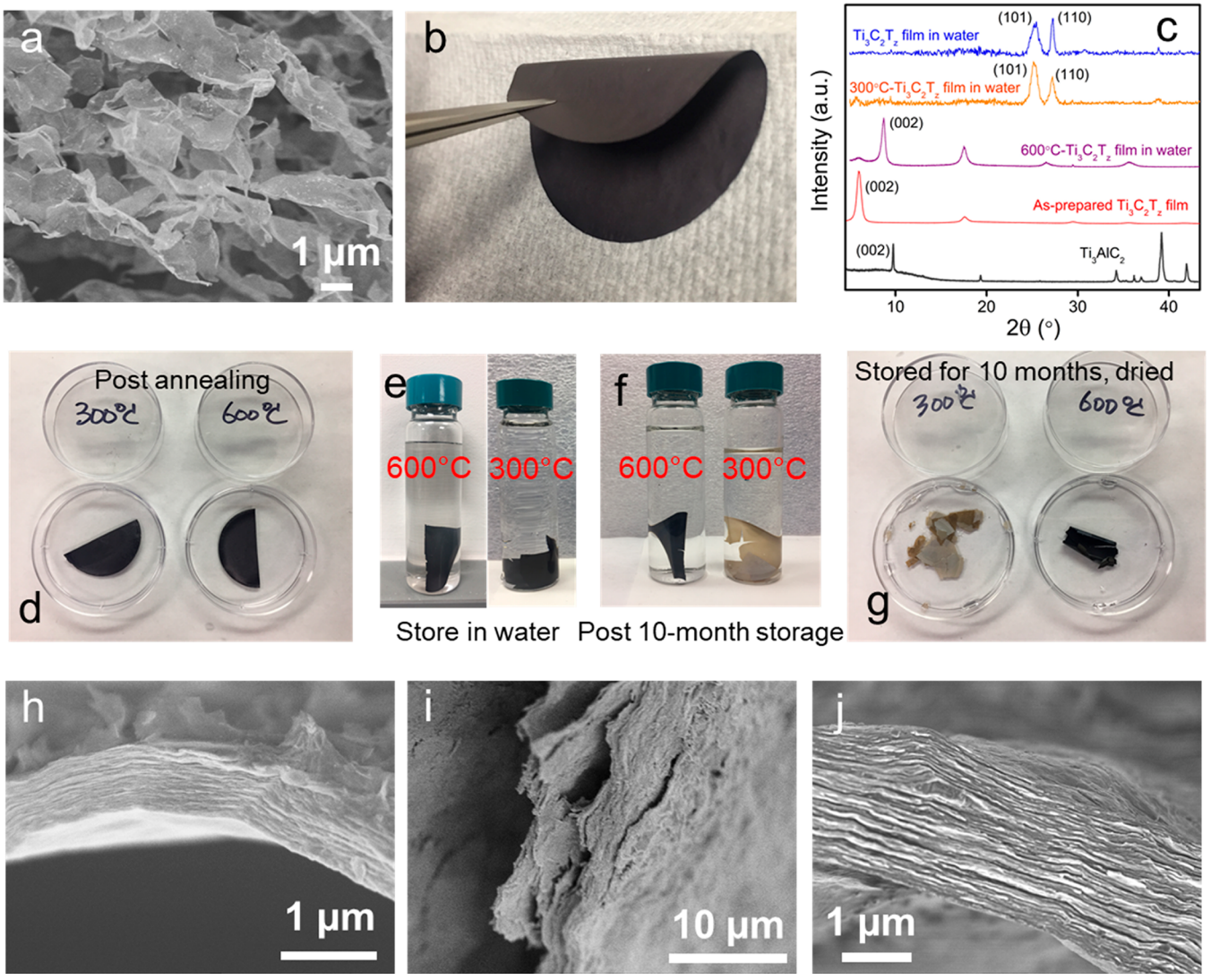

Figure 2. (a) Morphology of freeze-dried $Ti_3C_2T_z$ nanosheets by scanning electron microscopy (SEM) and (b) freestanding $Ti_3C_2T_z$ film made by vacuum filtration; (c) X-ray diffraction (XRD) spectra of Ti_3AlC_2 MAX phase particles, as-prepared film made by nanosheets prior to annealing, and annealed MXene films subject to 10 month storage in water. Images of (d) films after annealing at 300 and 600 °C, (e) annealed films in water after 24 h, (f) films stored in water after 10 months, and (g) annealed, stored films after being dried. Cross-section images for (h) as-prepared MXene film, (i) film annealed at 300 °C and then stored in water for 10 months, and (j) film annealed at 600 °C and then stored in water for 10 months.

be stable for over 10 months in water without any changes in synthesis recipes and introducing any antioxidation additives.

The cross-sectional SEM image of a film annealed at 600 °C and then stored for 10 months in water appears similar to the as-prepared film displaying a layered structure (Figure 2h,j and Figure S2). However, the film annealed at 300 °C changed from a layered structure of stacked nanosheets to an amorphous structure after long-term storage in water (Figure 2i).

The surface morphology of $Ti_3C_2T_z$ film after being annealed at 300 °C and stored in water for 10 months exhibited an amorphous nature with large aggregates present (Figure S3). In contrast, stacked nanosheets were observed on surface of the film annealed at 600 °C and stored at the same conditions. We next compare the surface of 600 °C-annealed film before and after 10 month storage; Figure S3f shows that the surface of the stacked nanosheets are covered with 30−60 nm hills, which were not visible on the as-prepared (Figure S3a) and 300 °C-annealed films (Figure S3b).

In addition, the effect of annealing on individual $Ti_3C_2T_z$ nanosheets was investigated. The nanosheets were first drop-cast and dried on a plasma-treated mica disc and then annealed at 550 °C. Atomic force microscopy (AFM) suggested that small bumps 3−9 nm in height formed on annealed nanosheets (shown in Figure S4). In contrast, as-prepared nanosheets exhibited cleaner surfaces without bumps. This indicated that some TiO_2 particles may form on the nanosheets during high-temperature annealing even in an inert atmosphere.

X-ray photoelectron spectroscopy (XPS) was used to measure changes in the MXene film surface chemistry after annealing and 10 month storage in water. The survey spectra and surface elemental compositions obtained by XPS are displayed in Figure S5 and Table S1. After being annealed at 300 °C, the high-resolution spectra of Ti 2p and C 1s did not vary much from the as-prepared films, except for a slight increase of Ti(IV) content (around 5 at. %), shown in Figure 3a,b. The slight oxidation may be caused by the reaction between the debonded surface water and Ti−C. After 10

https://dx.doi.org/10.1021/acsanm.0c02473
ACS Appl. Nano Mater. 2020, 3, 10578−10585

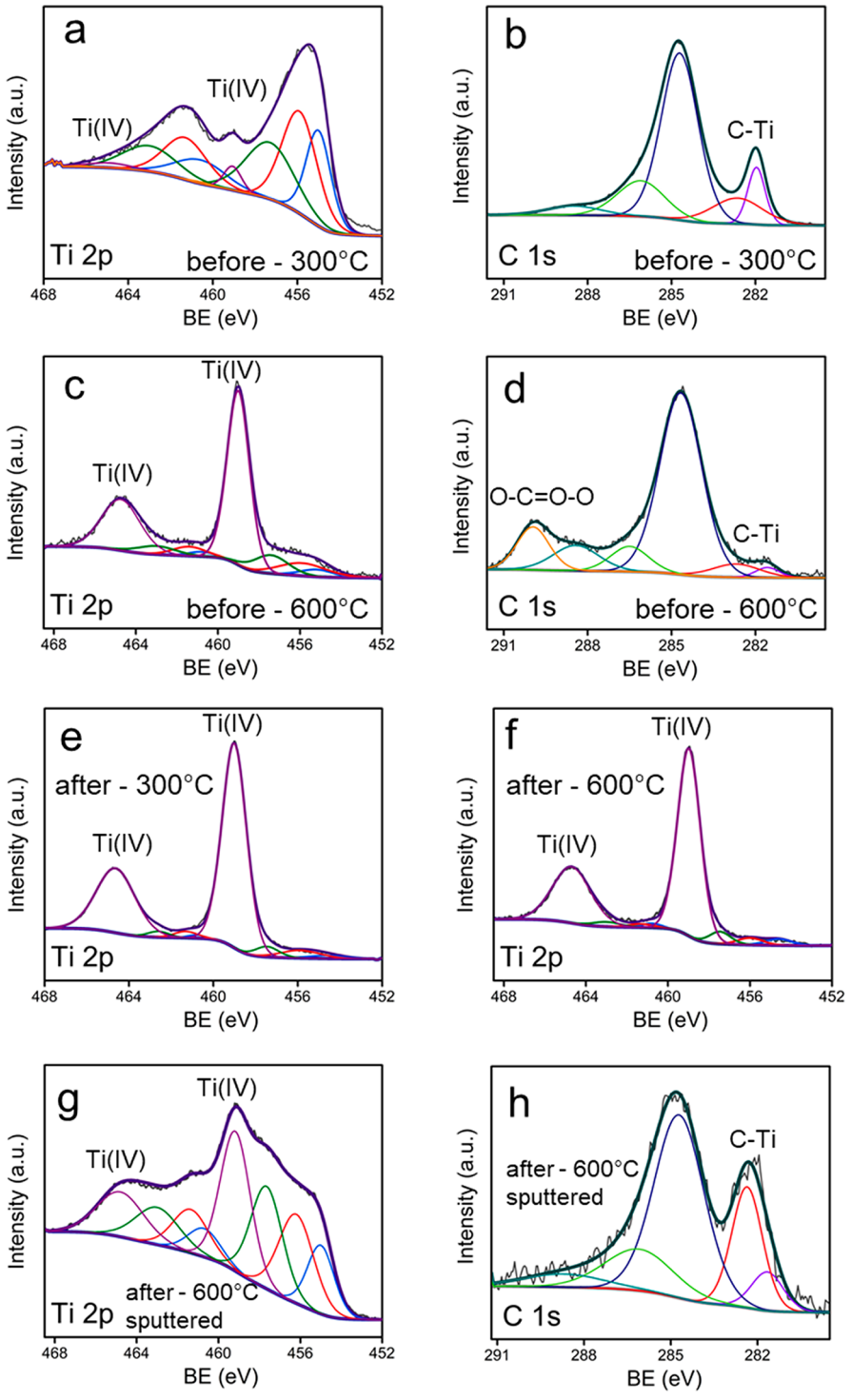

Figure 3. Ti 2p and C 1s spectra obtained by X-ray photoelectron spectroscopy (XPS) analysis for (a, b) $Ti_3C_2T_z$ film annealed at 300 °C, (c, d) $Ti_3C_2T_z$ film annealed at 600 °C, (e) 300 °C-annealed $Ti_3C_2T_z$ film after 10 month storage in water, (f) 600 °C-annealed $Ti_3C_2T_z$ film after 10 month storage in water, and (g, h) Ti 2p and C 1s spectra of the same film tested in panel f after being sputtered for 20 min by Ar^+ at a current of 15 mA.

month storage in water, films annealed at 300 °C were completely oxidized, as it is indicated by the rise of Ti(IV) component percentage from 23.1 to 88.1 at. % and the disappearance of the C−Ti−T_z peak (shown in Figure 3e and Figure S6). Combined with the evidence of the films' color change, these data suggest that the films annealed at 300 °C were completely oxidized and degraded after the 10 month storage in water.

XPS suggests that the surface of MXene films was severely oxidized after being annealed at 600 °C by showing a Ti(IV) content of 56.0 at. % and decreased C−Ti−T_z content in Figure 3c,d. Titanium carbonates (-O−C═O−O-) were also observed after 600 °C annealing, suggested by a pronounced peak at around 290 eV. The Ti(IV) content increased even more to 87.0 at. % after the 10 month storage in water. In addition, films annealed at 600 °C showed relatively

https://dx.doi.org/10.1021/acsanm.0c02473
ACS Appl. Nano Mater. 2020, 3, 10578−10585

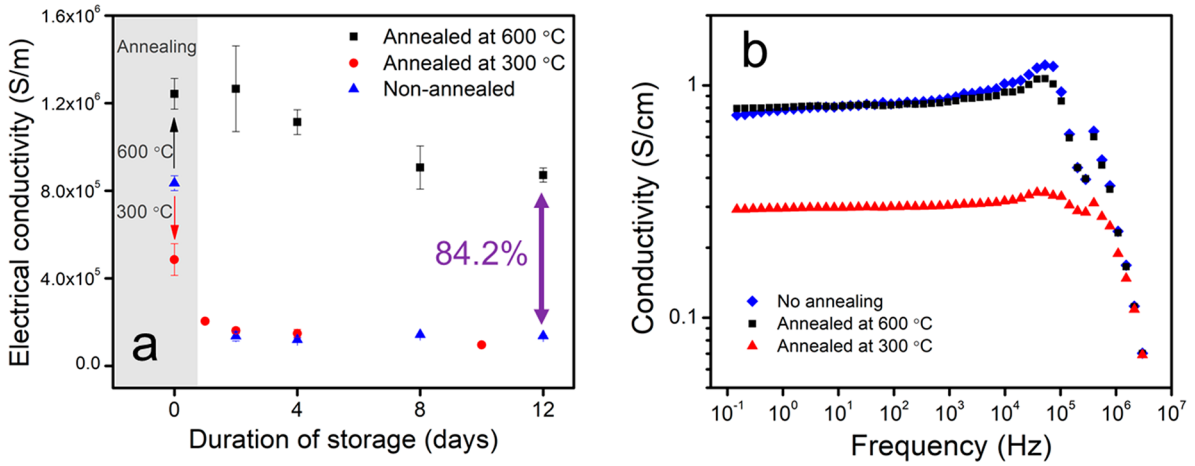

Figure 4. (a) Electronic conductivities of $Ti_3C_2T_z$ film before and after being annealed at 300 and 600 °C and then stored for consecutive days in a humidity-controlled chamber at 80% RH; (b) frequency dependence of the AC conductivities measured by dielectric spectroscopy.

unchanged Ti, C, and O compositions before and after the long storage (indicated in Table S1). In combination with prior SEM observations, the results indicate that a surface layer of TiO_2 formed uniformly after the 600 °C annealing step. Since the system was purged with inert gas, the formation of TiO_2 and carbonates is more likely caused by the oxidation reaction from surface attached H_2O molecules and O-containing functional radicals.

However, the oxidation of a 600 °C-annealed film surface as indicated by XPS is not obvious in the unchanged visible appearance of the film. Since XPS is limited to characterizing only the topmost surface of the films, the removal of the film top layer is needed to determine the interior film composition. Argon sputtering was used to remove the outmost layer of the stored MXene film annealed at 600 °C. The interior composition of the film was much less oxidized, indicated by a significant drop of Ti(IV) content from 87.0 to 33.0 at. % in Ti 2p XPS spectra before and after Ar sputtering for 20 min. In addition, pronounced C−Ti−T_z peaks (with binding energy of 281.6 and 282.4 eV) reappeared after sputtering, as it is shown in Figure 3h. The chemical composition of Ti(IV) of the sputtered sample may be even lower since Ar sputtering that etched the surface layer, at the same time, could also have mixed some surface TiO_2 components into the interior region, depending on the ion current and time applied in the sputtering. Sputtering at a reduced duration resulted in a relatively higher TiO_2 composition, while longer sputtering time leads to lower Ti(IV) content, as it is shown in Figure S7. XPS results also suggest that a layer of TiO_2 formed on the film surface when the sample was annealed at 600 °C; however, the protected interior part of the film did not show severe oxidation even after 10 months of being in contact with water.

To better characterize the difference in the degree of oxidation between the $Ti_3C_2T_z$ film's surface and interior structure of the film, elemental analysis was conducted by energy dispersive X-ray spectroscopy (EDS), shown in Figure S8. The elemental mappings of oxygen and titanium are displayed in Figure S9. The extent of oxidation was determined by oxygen content in the defined regions of the film cross-section. The oxygen content in the region close to the surface of the film was calculated to be 45.4 wt %, much higher than 25.6 wt % in the interior of the film. In addition, the titanium percentage of the interior region was 51.6 wt %, which was higher than the surface layers at 36.2 wt %. The elemental contents of fluorine and chlorine are also found to be higher in the interior region than close to the film surface. Our findings with EDS confirm that the MXene film was more oxidized on the surface, while $Ti_3C_2T_z$ was mostly retained in the film interior.

The oxidation layer formed on the film's surface was also confirmed by the surface wetting behaviors. Figure S10 shows that after being annealed at 300 °C, the contact angle of water on the film increased from 60° to 74°, indicating increased surface hydrophobicity. This may be caused by the loss of surface terminal groups and bonded water during annealing. However, the film annealed at 600 °C exhibits a much smaller contact angle of 28°. This suggests that the film surface turns hydrophilic with the formation of a TiO_2 layer at the elevated temperature.

On the basis of XPS and EDS results, we propose that the dense TiO_2 layer covering the film's surface may act as barriers preventing water ingress and oxidation in the interior. However, there are difficulties in determining these surface property changes experimentally, which need to be addressed in future work. In addition, XRD suggests that annealing MXene films at elevated temperatures may cause the stacked nanosheets to form a more compact packing, which could be another obstacle for water permeation and oxidation. This is consistent with prior reports.[14,38] Another possibility for the enhanced stability of 600 °C annealed film is reduction of the number of oxygen-containing groups in the films. This is indicated by the decreased content of Ti−O_x, Ti−OH, and bonded H_2O in O 1s XPS spectra shown in Figure S11 and Table S2.

We next investigated how thermal annealing and storage change the electrical properties of $Ti_3C_2T_z$ films (Figure 4). The electrical conductivity was found decreased after 300 °C annealing but increased after 600 °C annealing. First, the increased film conductivity after 600 °C annealing may be caused by the reduced amount of oxygen-containing functional groups attached to the MXene surface. Berdiyorov and Jiang et al. reported that a considerable reduction of the electronic transmission can be caused by the terminated oxygen-containing groups.[39,40] Attached functional groups may have electron-withdrawing ability which prevents the electronic transmission within nanosheets,[41] so removal of these oxygen-

https://dx.doi.org/10.1021/acsanm.0c02473
ACS Appl. Nano Mater. 2020, 3, 10578−10585

containing groups via high-temperature annealing (at 600 °C) will accelerate the electronic transmission. In addition, suggested by reduced *d*-spacing of MXene flakes after annealing, more compact MXene films may cause faster electronic transmission due to more nanosheets overlaps and contacts. The stability of MXene film conductivity is also investigated. When stored in a chamber with controlled humidity at 80% RH (high humidity is used to shorten the experimental duration), the film annealed at 600 °C exhibited more stable conductivities than both the as-prepared and 300 °C annealed samples shown in Figure 4a.

We also investigated the frequency-dependent AC conductivity in the annealed films' cross-section direction by dielectric spectroscopy, from 0.1 Hz to 10 MHz. The results (Figure 4b) show that the $Ti_3C_2T_z$ film annealed at 300 °C exhibited the lowest conductivity. However, the as-prepared and 600 °C annealed $Ti_3C_2T_z$ films exhibited higher conductivity and show similar electronic properties. This suggests that the TiO_2 layer induced in annealing is thin and does not affect the electrical properties of the MXene film. In addition, despite the existence of the thin oxidized surface layers, the AC conductivity of 600 °C annealed film was retained due to the more compact surface structure and reduced amount of electron-withdrawing surface functionalities.

Radio-frequency (RF)-induced heating can also be used to quantify the interactions between the MXene films and electromagnetic waves; this heating response is correlated with the structure and AC bulk conductivities of the samples.[42] Figure S12 shows the dynamic thermal response of these structures; again, the 600 °C annealed films (before storage in water) showed a response similar to the as-prepared structure, whereas the plateau temperature for the 300 °C annealed films is far lower, indicating a loss of conductivity.

Our study demonstrates that annealing $Ti_3C_2T_z$ films at elevated temperatures such as 600 °C helps to prevent film degradation, even for films stored in water for over a 10-month period. This method significantly extends the oxidation resistance of $Ti_3C_2T_z$ MXene films, which may be potentially used as functional coatings, electrodes in batteries and supercapacitors, membranes, and catalytic surfaces and may broaden the durable application of MXene devices in aqueous environments.

■ ASSOCIATED CONTENT

Supporting Information

The Supporting Information is available free of charge at https://pubs.acs.org/doi/10.1021/acsanm.0c02473.

Materials and methods in which the sample preparation steps and material characterization are elaborated, also including supporting figures and images (PDF)

■ AUTHOR INFORMATION

Corresponding Authors

Micah J. Green − *Artie McFerrin Department of Chemical Engineering and Department of Materials Science and Engineering, Texas A&M University, College Station, Texas 77843, United States;* orcid.org/0000-0001-5691-0861; Email: micah.green@tamu.edu

Miladin Radovic − *Department of Materials Science and Engineering, Texas A&M University, College Station, Texas 77843, United States*; Email: mradovic@tamu.edu

Jodie L. Lutkenhaus − *Artie McFerrin Department of Chemical Engineering and Department of Materials Science and Engineering, Texas A&M University, College Station, Texas 77843, United States;* orcid.org/0000-0002-2613-6016; Email: jodie.lutkenhaus@tamu.edu

Authors

Xiaofei Zhao − *Artie McFerrin Department of Chemical Engineering, Texas A&M University, College Station, Texas 77843, United States;* orcid.org/0000-0002-0593-8490

Dustin E. Holta − *Department of Materials Science and Engineering, Texas A&M University, College Station, Texas 77843, United States*

Zeyi Tan − *Department of Materials Science and Engineering, Texas A&M University, College Station, Texas 77843, United States*

Ju-Hyun Oh − *Artie McFerrin Department of Chemical Engineering, Texas A&M University, College Station, Texas 77843, United States*

Ian J. Echols − *Artie McFerrin Department of Chemical Engineering, Texas A&M University, College Station, Texas 77843, United States*

Muhammad Anas − *Artie McFerrin Department of Chemical Engineering, Texas A&M University, College Station, Texas 77843, United States*

Huaixuan Cao − *Artie McFerrin Department of Chemical Engineering, Texas A&M University, College Station, Texas 77843, United States*

Complete contact information is available at: https://pubs.acs.org/10.1021/acsanm.0c02473

Notes

The authors declare no competing financial interest.

■ ACKNOWLEDGMENTS

This work is funded by the U.S. National Science Foundation (Grant CMMI-1760859). We acknowledge Dr. Mustafa Akbulut's group at Texas A&M University for assistance in use of their interfacial wettability instrument. We acknowledge the TAMU Materials Characterization Facility (MCF) for the AFM, XPS, and SEM-EDS analyses and TAMU Department of Chemistry for use of XRD. We are thankful for the guidance on XPS analysis from Dr. Jing Wu in the Materials Characterization Facility at TAMU.

■ REFERENCES

(1) Anayee, M.; Kurra, N.; Alhabeb, M.; Seredych, M.; Hedhili, M. N.; Emwas, A.-H.; Alshareef, H. N.; Anasori, B.; Gogotsi, Y. Role of acid mixtures etching on the surface chemistry and sodium ion storage in Ti3C2Tx MXene. *Chem. Commun.* **2020**, *56* (45), 6090−3.

(2) Anasori, B.; Lukatskaya, M. R.; Gogotsi, Y. 2D metal carbides and nitrides (MXenes) for energy storage. *Nat. Rev. Mater.* **2017**, *2*, 16098.

(3) Anasori, B.; Xie, Y.; Beidaghi, M.; Lu, J.; Hosler, B. C.; Hultman, L.; Kent, P. R. C.; Gogotsi, Y.; Barsoum, M. W. Two-Dimensional, Ordered, Double Transition Metals Carbides (MXenes). *ACS Nano* **2015**, *9* (10), 9507−16.

(4) Mashtalir, O.; Naguib, M.; Mochalin, V. N.; Dall'Agnese, Y.; Heon, M.; Barsoum, M. W.; Gogotsi, Y. Intercalation and delamination of layered carbides and carbonitrides. *Nat. Commun.* **2013**, *4*, 1716.

(5) Naguib, M.; Mashtalir, O.; Carle, J.; Presser, V.; Lu, J.; Hultman, L.; Gogotsi, Y.; Barsoum, M. W. Two-Dimensional Transition Metal Carbides. *ACS Nano* **2012**, *6* (2), 1322−31.

(6) Maleski, K.; Alhabeb, M. Top-Down MXene Synthesis (Selective Etching). In*2D Metal Carbides and Nitrides (MXenes): Structure, Properties and Applications*; Anasori, B, Gogotsi, Y, Eds.; Springer International: Cham, Switzerland, 2019; pp 69−87, DOI: 10.1007/978-3-030-19026-2_5.
(7) Alhabeb, M.; Maleski, K.; Anasori, B.; Lelyukh, P.; Clark, L.; Sin, S.; Gogotsi, Y. Guidelines for Synthesis and Processing of Two-Dimensional Titanium Carbide (Ti3C2Tx MXene). *Chem. Mater.* **2017**, *29* (18), 7633−44.
(8) Naguib, M.; Kurtoglu, M.; Presser, V.; Lu, J.; Niu, J.; Heon, M.; Hultman, L.; Gogotsi, Y.; Barsoum, M. W. Two-Dimensional Nanocrystals Produced by Exfoliation of Ti3AlC2. *Adv. Mater.* **2011**, *23* (37), 4248−53.
(9) Naguib, M.; Mochalin, V. N.; Barsoum, M. W.; Gogotsi, Y. 25th Anniversary Article: MXenes: A New Family of Two-Dimensional Materials. *Adv. Mater.* **2014**, *26* (7), 992−1005.
(10) Shah, S. A.; Habib, T.; Gao, H.; Gao, P.; Sun, W.; Green, M. J.; Radovic, M. Template-free 3D titanium carbide (Ti3C2Tx) MXene particles crumpled by capillary forces. *Chem. Commun.* **2017**, *53* (2), 400−3.
(11) Sun, W.; Shah, S. A.; Chen, Y.; Tan, Z.; Gao, H.; Habib, T.; Radovic, M.; Green, M. J. Electrochemical etching of Ti2AlC to Ti2CTx (MXene) in low-concentration hydrochloric acid solution. *J. Mater. Chem. A* **2017**, *5* (41), 21663−8.
(12) VahidMohammadi, A.; Mojtabavi, M.; Caffrey, N. M.; Wanunu, M.; Beidaghi, M. Assembling 2D MXenes into Highly Stable Pseudocapacitive Electrodes with High Power and Energy Densities. *Adv. Mater.* **2019**, *31* (8), 1806931.
(13) Er, D.; Li, J.; Naguib, M.; Gogotsi, Y.; Shenoy, V. B. Ti3C2MXene as a High Capacity Electrode Material for Metal (Li, Na, K Ca) Ion Batteries. *ACS Appl. Mater. Interfaces* **2014**, *6* (14), 11173−9.
(14) Sarycheva, A.; Polemi, A.; Liu, Y.; Dandekar, K.; Anasori, B.; Gogotsi, Y. 2D titanium carbide (MXene) for wireless communication. *Science Advances* **2018**, *4* (9), No. eaau0920.
(15) Shahzad, F.; Alhabeb, M.; Hatter, C. B.; Anasori, B.; Hong, S. M.; Koo, C. M.; Gogotsi, Y. Electromagnetic interference shielding with 2D transition metal carbides (MXenes). *Science* **2016**, *353* (6304), 1137−40.
(16) Ding, L.; Wei, Y.; Li, L.; Zhang, T.; Wang, H.; Xue, J.; Ding, L.-X.; Wang, S.; Caro, J.; Gogotsi, Y. MXene molecular sieving membranes for highly efficient gas separation. *Nat. Commun.* **2018**, *9* (1), 155.
(17) Weng, G.-M.; Mariano, M.; Lipton, J.; Taylor, A. D. MXene Films, Coatings, and Bulk Processing. In*2D Metal Carbides and Nitrides (MXenes): Structure, Properties and Applications*; Anasori, B, Gogotsi, Y, Eds.; Springer International: Cham, Switzerland, 2019; pp 197−219, DOI: 10.1007/978-3-030-19026-2_12.
(18) An, H.; Habib, T.; Shah, S.; Gao, H.; Radovic, M.; Green, M. J.; Lutkenhaus, J. L. Surface-agnostic highly stretchable and bendable conductive MXene multilayers. *Science Advances* **2018**, *4* (3), No. eaaq0118.
(19) Habib, T.; Zhao, X.; Shah, S. A.; Chen, Y.; Sun, W.; An, H.; Lutkenhaus, J. L.; Radovic, M.; Green, M. J. Oxidation stability of Ti3C2Tx MXene nanosheets in solvents and composite films. *npj 2D Mater. Appl.* **2019**, *3* (1), 8.
(20) Chae, Y.; Kim, S. J.; Cho, S.-Y.; Choi, J.; Maleski, K.; Lee, B.-J.; Jung, H.-T.; Gogotsi, Y.; Lee, Y.; Ahn, C. W. An investigation into the factors governing the oxidation of two-dimensional Ti3C2MXene. *Nanoscale* **2019**, *11* (17), 8387−93.
(21) Huang, S.; Mochalin, V. N. Hydrolysis of 2D Transition-Metal Carbides (MXenes) in Colloidal Solutions. *Inorg. Chem.* **2019**, *58* (3), 1958−66.
(22) Zhang, C. J.; Pinilla, S.; McEvoy, N.; Cullen, C. P.; Anasori, B.; Long, E.; Park, S.-H.; Seral-Ascaso, A.; Shmeliov, A.; Krishnan, D.; Morant, C.; Liu, X.; Duesberg, G. S.; Gogotsi, Y.; Nicolosi, V. Oxidation Stability of Colloidal Two-Dimensional Titanium Carbides (MXenes). *Chem. Mater.* **2017**, *29* (11), 4848−56.
(23) Lee, Y.; Kim, S. J.; Kim, Y.-J.; Lim, Y.; Chae, Y.; Lee, B.-J.; Kim, Y.-T.; Han, H.; Gogotsi, Y.; Ahn, C. W. Oxidation-resistant titanium carbide MXene films. *J. Mater. Chem. A* **2020**, *8* (2), 573−81.
(24) Lipatov, A.; Alhabeb, M.; Lukatskaya, M. R.; Boson, A.; Gogotsi, Y.; Sinitskii, A. Effect of Synthesis on Quality, Electronic Properties and Environmental Stability of Individual Monolayer Ti3C2MXene Flakes. *Advanced Electronic Materials.* **2016**, *2* (12), 1600255.
(25) Carey, M.; Hinton, Z.; Natu, V.; Pai, R.; Sokol, M.; Alvarez, N. J.; Kalra, V.; Barsoum, M. W. Dispersion and Stabilization of Alkylated 2D MXene in Nonpolar Solvents and Their Pseudocapacitive Behavior. *Cell Reports Physical Science.* **2020**, *1* (4), 100042.
(26) Maleski, K.; Mochalin, V. N.; Gogotsi, Y. Dispersions of Two-Dimensional Titanium Carbide MXene in Organic Solvents. *Chem. Mater.* **2017**, *29* (4), 1632−40.
(27) Wu, X.; Wang, Z.; Yu, M.; Xiu, L.; Qiu, J. Stabilizing the MXenes by Carbon Nanoplating for Developing Hierarchical Nanohybrids with Efficient Lithium Storage and Hydrogen Evolution Capability. *Adv. Mater.* **2017**, *29* (24), 1607017.
(28) Zhao, X.; Vashisth, A.; Prehn, E.; Sun, W.; Shah, S. A.; Habib, T.; Chen, Y.; Tan, Z.; Lutkenhaus, J. L.; Radovic, M.; Green, M. J. Antioxidants Unlock Shelf-Stable Ti3C2Tx (MXene) Nanosheet Dispersions. *Matter.* **2019**, *1* (2), 513−26.
(29) Natu, V.; Hart, J. L.; Sokol, M.; Chiang, H.; Taheri, M. L.; Barsoum, M. W. Edge Capping of 2D-MXene Sheets with Polyanionic Salts To Mitigate Oxidation in Aqueous Colloidal Suspensions. *Angew. Chem.* **2019**, *131* (36), 12785−90.
(30) Mashtalir, O.; Naguib, M.; Mochalin, V. N.; Dall'Agnese, Y.; Heon, M.; Barsoum, M. W.; Gogotsi, Y. Intercalation and delamination of layered carbides and carbonitrides. *Nat. Commun.* **2013**, *4* (1), 1716.
(31) Shuck, C. E.; Han, M.; Maleski, K.; Hantanasirisakul, K.; Kim, S. J.; Choi, J.; Reil, W. E. B.; Gogotsi, Y. Effect of Ti3AlC2MAX Phase on Structure and Properties of Resultant Ti3C2Tx MXene. *ACS Applied Nano Materials.* **2019**, *2* (6), 3368−76.
(32) Hart, J. L.; Hantanasirisakul, K.; Lang, A. C.; Anasori, B.; Pinto, D.; Pivak, Y.; van Omme, J. T.; May, S. J.; Gogotsi, Y.; Taheri, M. L. Control of MXenes' electronic properties through termination and intercalation. *Nat. Commun.* **2019**, *10* (1), 522.
(33) Persson, I.; Näslund, L-Å; Halim, J.; Barsoum, M. W.; Darakchieva, V.; Palisaitis, J.; Rosen, J.; Persson, P. O. Å. On the organization and thermal behavior of functional groups on Ti 3 C 2 MXene surfaces in vacuum. *2D Mater.* **2018**, *5* (1), 015002.
(34) Huang, H.; Song, Y.; Li, N.; Chen, D.; Xu, Q.; Li, H.; He, J.; Lu, J. One-step in-situ preparation of N-doped TiO2@C derived from Ti3C2MXene for enhanced visible-light driven photodegradation. *Appl. Catal., B* **2019**, *251*, 154−61.
(35) Gao, Y.; Chen, H.; Zhou, A.; Li, Z.; Liu, F.; Hu, Q.; Wang, L. Novel Hierarchical TiO2/C Nanocomposite with Enhanced Photocatalytic Performance. *Nano* **2015**, *10* (05), 1550064.
(36) Wang, Y.; Li, T.; Ma, P.; Zhang, S.; Zhang, H.; Du, M.; Xie, Y.; Chen, M.; Dong, W.; Ming, W. Artificial Nacre from Supramolecular Assembly of Graphene Oxide. *ACS Nano* **2018**, *12* (6), 6228−35.
(37) Li, D.; Müller, M. B.; Gilje, S.; Kaner, R. B.; Wallace, G. G. Processable aqueous dispersions of graphene nanosheets. *Nat. Nanotechnol.* **2008**, *3* (2), 101−5.
(38) Osti, N. C.; Naguib, M.; Ostadhossein, A.; Xie, Y.; Kent, P. R. C.; Dyatkin, B.; Rother, G.; Heller, W. T.; van Duin, A. C. T.; Gogotsi, Y.; Mamontov, E. Effect of Metal Ion Intercalation on the Structure of MXene and Water Dynamics on its Internal Surfaces. *ACS Appl. Mater. Interfaces* **2016**, *8* (14), 8859−63.
(39) Jiang, X.; Kuklin, A. V.; Baev, A.; Ge, Y.; Ågren, H.; Zhang, H.; Prasad, P. N. Two-dimensional MXenes: From morphological to optical, electric, and magnetic properties and applications. *Phys. Rep.* **2020**, *848*, 1−58.
(40) Berdiyorov, G. R. Effect of surface functionalization on the electronic transport properties of Ti 3 C 2 MXene. *EPL (Europhysics Letters).* **2015**, *111* (6), 67002.

https://dx.doi.org/10.1021/acsanm.0c02473
ACS Appl. Nano Mater. 2020, 3, 10578−10585

(41) Lioi, D. B.; Neher, G.; Heckler, J. E.; Back, T.; Mehmood, F.; Nepal, D.; Pachter, R.; Vaia, R.; Kennedy, W. J. Electron-Withdrawing Effect of Native Terminal Groups on the Lattice Structure of Ti3C2Tx MXenes Studied by Resonance Raman Scattering: Implications for Embedding MXenes in Electronic Composites. *ACS Applied Nano Materials.* **2019**, *2* (10), 6087−91.
(42) Habib, T.; Patil, N.; Zhao, X.; Prehn, E.; Anas, M.; Lutkenhaus, J. L.; Radovic, M.; Green, M. J. Heating of Ti3C2Tx MXene/polymer composites in response to Radio Frequency fields. *Sci. Rep.* **2019**, *9* (1), 16489.

https://dx.doi.org/10.1021/acsanm.0c02473
ACS Appl. Nano Mater. 2020, 3, 10578−10585